

Dynamic Stabilization of a Microring Modulator Under Thermal Perturbation

Kishore Padmaraju¹, Johnnie Chan¹, Long Chen², Michal Lipson², Keren Bergman¹

1: Department of Electrical Engineering, Columbia University, 500 West 120th Street, New York, New York 10027, USA

2: School of Electrical and Computer Engineering, Cornell University, 428 Phillips Hall, Ithaca, New York 14853, USA
kpadmara@ee.columbia.edu

Abstract: We demonstrate the first active stabilization of a microring-based device within a thermally volatile environment. The proposed design is CMOS integratable and leverages low-speed power monitoring and a feedback loop circuit for dynamic thermal correction.

OCIS codes: (230.4110) Modulators; (230.4555) Coupled Resonators; (200.4650) Optical Interconnects.

1. Introduction

Microring-based nanophotonic devices have the ability to resolve the bandwidth-density challenges facing future multi-core processors. The resonance characteristics of microrings can be utilized to create modulators, filters, switches, and detectors that are ideal for wavelength-division-multiplexing (WDM) based photonic networks-on-chip. Several architectures utilizing microring-based devices in this capacity have already been proposed [1,2]. However, the WDM-enabling wavelength selectivity of microrings also causes them to be extremely vulnerable to changes in temperature. As shown in this experiment, temperature changes on the order of ~1K are enough to significantly shift the operating wavelength of the microring, and thus render the device inoperable.

Current attempts to resolve the thermal sensitivity of passive and active microring-based devices have been focused on creating thermally insensitive structures [3], integrated temperature monitoring structures [4], or dynamic feedback systems [5]. However, to date, none of these attempts have demonstrated operation of an active microring-based device in a thermally volatile environment representative of an operational microelectronic system.

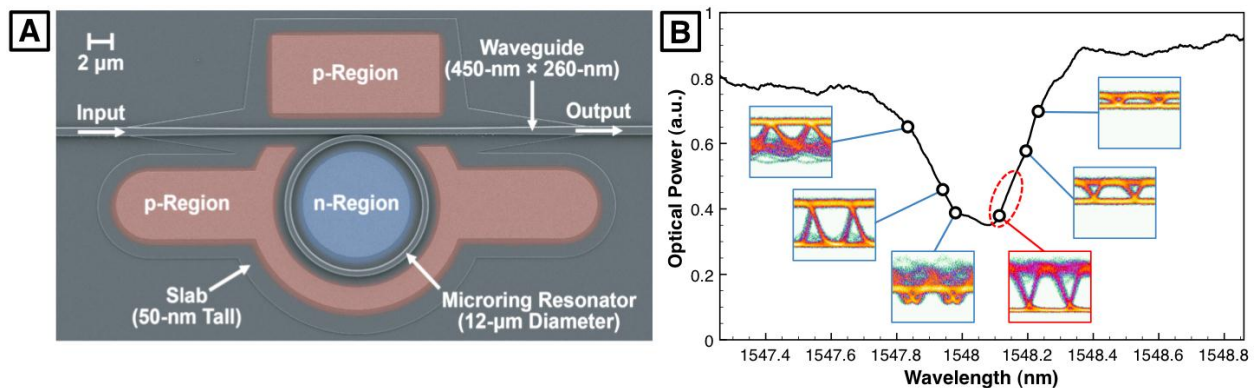


Figure 1: a) Scanning-electron-microscope (SEM) image of the microring modulator. b) Experimentally measured mean power of the modulated signal, with the region of optimum modulation indicated in dashed red. Inset eye-diagrams elucidate the varying optical output caused by wavelength shifts (temperature change has the equivalency of a wavelength shift for a microring).

In this experiment, we consider a silicon microring modulator (Fig. 1a). The regions surrounding the ring are doped appropriately to create a diode structure, allowing carrier injection into the optical waveguide. The corresponding free carrier dispersion effects shifts the resonant wavelength, enabling high-speed modulation. Optimum operation of the silicon microring modulator is traditionally achieved with a small forward bias current [6]. Due to the significant amounts of heat generated by carrier recombination in the diode junction, the forward bias current has the ancillary effect of shifting the operating wavelength of the microring modulator. Hence, the bias current can be reduced or increased to cool or heat, respectively, the microring, thus counteracting thermal fluctuations in the ambient environment. This method has been shown to be effective for a range of up to 15 K, and twice as energy efficient as using a separate resistive heating element [7]. We utilize this effective and efficient tuning mechanism to dynamically control the operating wavelength of the microring modulator as it experiences external thermal perturbations.

To use the aforementioned tuning mechanism appropriately in a feedback loop, a monitoring mechanism is needed to ascertain the direction of wavelength shift caused by the thermal perturbation. Our system monitors the mean optical power of the modulated signal, which is sufficient for determining the direction and magnitude of the thermal drift of the microring modulator. This principle is clarified in Fig. 1b, where the mean power of the modulated signal is measured versus wavelength. While in this instance, we are varying the operating wavelength,

varying the temperature will produce a similar curve. When the operating wavelength is at the appropriate wavelength, the on-off-keying (OOK) modulation intrinsically produces a decrease in the mean power of the modulated signal. The region of optimum modulation is indicated in Fig. 1b, in dashed red. Any deviation from this region is measured using our power-monitoring scheme, and using our feedback loop, a correction is made by adjustment of the bias current. Compared to the GHz-scale operation of the microring modulator, this solution is appropriately slower, operating on the same bandwidth-scale as thermal fluctuations.

2. Experiments and Results

The 6- μm -radius microring modulator used in this experiment was fabricated at the Cornell Nanofabrication Facility, with further details on the fabrication process found in [8]. In our experimental setup (Fig. 2), a pulsed-pattern-generator (PPG) was used to generate a 10-Gb/s non-return-to-zero (NRZ) 2^7 -1 pseudo-random bit sequence (PRBS) electrical signal. The 0.8- V_{pp} signal was biased at 0.55 V and conditioned with a pre-emphasis circuit to enable high-speed operation of the device [6]. A CW tunable laser was set to TE polarization before being launched onto the chip with a power of 6 dBm. Waveguide and coupling losses yielded a fiber-to-fiber loss of 20.4 dB. The OOK modulation produces additional loss, yielding a recovered power ranging from -14.4 dBm to -17.6 dBm, depending on the depth of the modulation. 10% of this microring-modulated signal was tapped for the power monitoring feedback. The remaining signal is then amplified and filtered before being sent to a PIN-TIA photodetector followed by a limiting amplifier (LA). A bit-error-rate tester (BERT) and variable optical attenuator (VOA) are used in conjunction for the BER measurements.

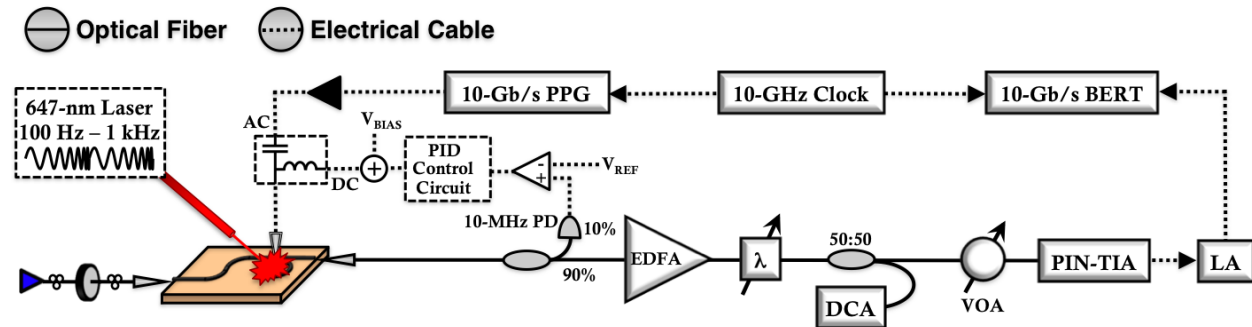


Figure 2: Experimental Setup.

As seen in Fig. 2, a visible laser at a wavelength of 647 nm was vertically aligned above the microring. This arrangement allowed a localized heating of the microring that did not disturb the optical power laterally coupling into and out of the chip, a crucial requirement of our power monitoring scheme. The visible laser was set to low-power CW operation, and focused on the microring while the wavelength and DC bias were set to ensure optimum modulation. Once the ideal modulation of the microring was established, the visible laser power was increased, and then internally modulated with a sinusoidal modulation. The modulation was continuously swept from 100 Hz to 1 kHz to demonstrate the validity of the feedback system at varying frequencies of thermal fluctuation. By following this procedure, we created an environment where the microring experienced both heating and cooling relative to its temperature of optimum modulation. By measuring the resonance shift of the microring modulator in its electrically passive state, we have calculated that a temperature fluctuation of ~ 4 K was produced.

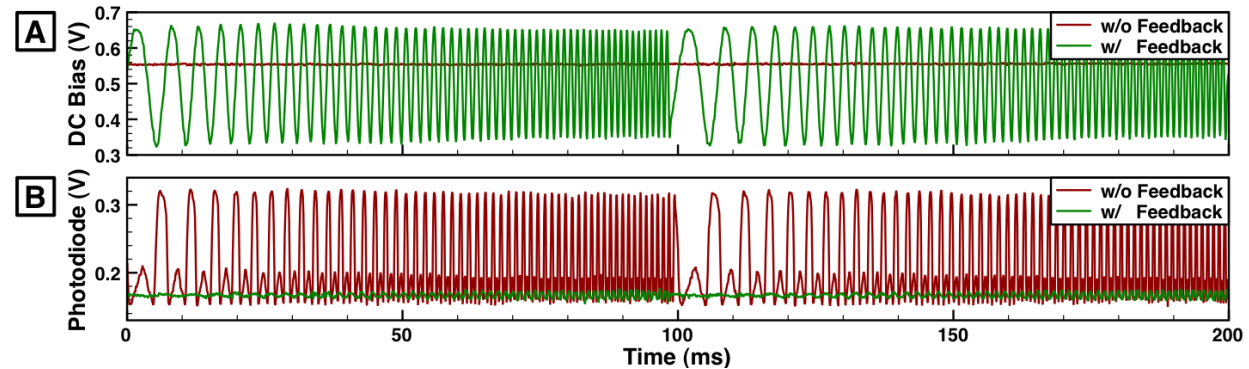


Figure 3: Oscilloscope measurements (with and without the feedback system) of the (a) DC bias applied, and the (b) photodiode voltage measuring the mean modulation power.

As shown in the experimental setup (Fig. 2), a photodiode with 10-MHz bandwidth was used to monitor the mean optical power of the modulation. The relatively slow photodiode is sufficient to track changes in the mean

optical power attributable to thermal fluctuations. The voltage from the photodiode is compared to a reference voltage using an INA129 instrumentation amplifier (20-MHz bandwidth). The error signal is then relayed to a proportional-integral-derivative (PID) controller composed of LF411 op-amps (3-MHz bandwidth). The feedback signal is then added to the bias voltage using a standard op-amp summing circuit.

The dynamic adjustment of the DC bias is illustrated in the oscilloscope trace of Fig. 3a. Without the feedback circuit, the DC bias is a constant 0.55 V, whereas, with the feedback circuit, the voltage is swung dynamically between 0.3 V and 0.7 V to correct for the thermal fluctuations. The effect of this action can be seen in the photodiode power (Fig. 3b), which was used to measure the mean modulation power for our feedback mechanism. Without the feedback circuit the mean modulation power fluctuates in correspondence with the thermal fluctuations. The feedback system locks the mean modulation power to the set reference, ensuring that the modulation is maintained throughout the duration of the thermal perturbation.

The eye diagrams and BER measurements in Fig. 4 validate the performance of the feedback system. Without thermal perturbation, there is a near negligible difference between operating the microring modulator without feedback (Fig. 4a), and with feedback (Fig. 4c), further confirmed by the 0.2-dB power penalty assessed by our BER measurements (Fig. 4e). As seen in Fig. 4b, subsection of the microring modulator to thermal perturbation without a corrective feedback system will result in catastrophic failure of the modulation. However, as can be seen in Fig. 4d, the feedback system can completely correct for the thermal disturbances, maintaining error-free modulation with a minimal power penalty of 0.4 dB (in comparison to the back-to-back case of Fig. 4a).

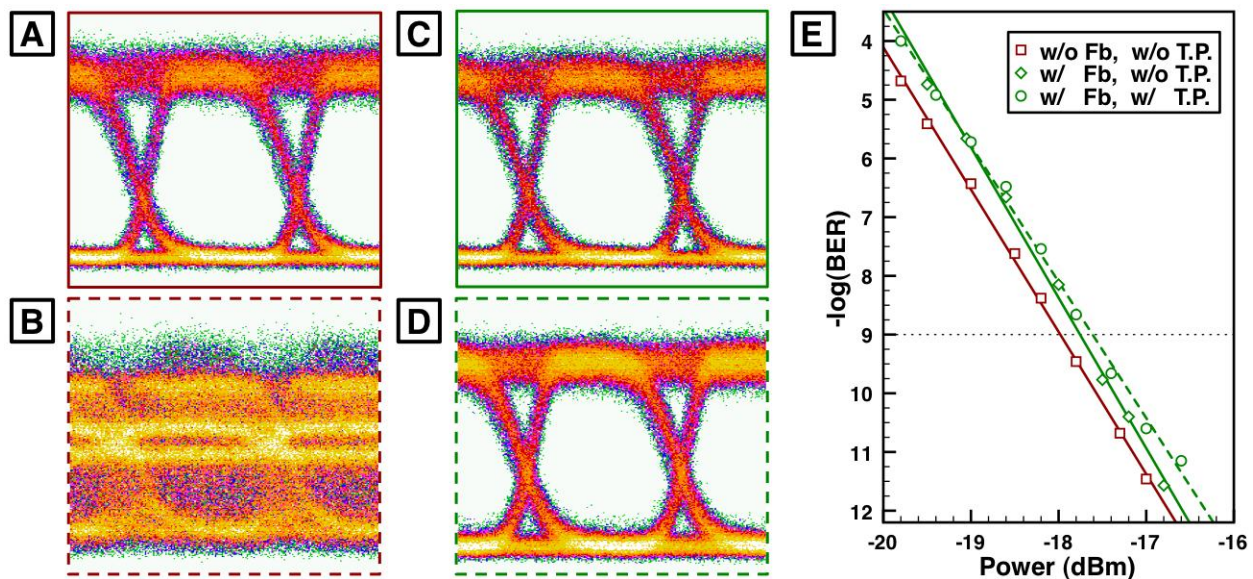


Figure 4: Eye diagrams of 10-Gb/s microring modulation *without* the feedback (Fb) system in (a) a stable thermal environment, and (b) under thermal perturbation (T.P.). Similarly, microring modulation *with* the feedback system in (c) a stable thermal environment, and (d) under thermal perturbation. (e) BER measurements corresponding to eye diagrams in (a), (c), and (d).

3. Conclusion

We have implemented a dynamic stabilization of a microring modulator using a feedback mechanism where only a small measurement of the mean optical power is necessary. As demonstrated, this bit-rate transparent technique can be implemented using much slower, and subsequently, energy efficient electronics. Finally, we note that the CMOS compatibility of a silicon microring modulator can be leveraged to integrate the demonstrated feedback system on the same fabrication level as the modulator itself.

This work was supported in part by the Interconnect Focus Center, one of five research centers funded under the Focus Center Research Program, a Semiconductor Research Corporation (SRC) and DARPA program, and by the National Science Foundation and SRC under grant ECCS-0903406 SRC Task 2001.

4. References

- [1] C. Batten, *et al.*, "Building many-core processor-to-DRAM networks with monolithic CMOS silicon photonics," *IEEE Micro* **29** (4) 8-21.
- [2] A. Shacham, *et al.*, "Photonic networks-on-chip for future generations of chip multiprocessors," *IEEE Trans. Comput.* **57** (9) 1246-1260.
- [3] B. Guha *et al.*, "CMOS-compatible athermal silicon microring resonators," *Opt. Express*. **18** (4) 3487-3493 (2010).
- [4] C. T. DeRose *et al.*, "Silicon microring modulator with integrated heater and temperature sensor for thermal control," *OFC*, (2010).
- [5] C. Qiu *et al.*, "Wavelength tracking with thermally controlled silicon resonators," *Opt. Express*. **19** (6) 5143-5148 (2011).
- [6] Q. Xu *et al.*, "12.5 Gbit/s carrier-injection-based silicon micro-ring silicon modulators," *Opt. Express*. **15** (2) 430-436 (2007).
- [7] S. Manipatruni *et al.*, "Wide temperature range operation of μm -scale silicon electro-optic modulators," *Opt. Lett.* **33** (19) 2185-2187. (2008).
- [8] L. Chen *et al.*, "Integrated GHz silicon photonic interconnect with μm -scale modulators and detectors," *Opt. Express*. **17** (17). (2009).